Real-time monitoring of different grinding phases in a disc mill

Abstract

We used the acceleration measurement of the grinding vessel for real-time monitoring of the grinding process in a disc mill. During grinding of clinker, we were able to identify three clearly distinguishable phases, i.e. breakage, plateau and agglomeration phase. In the breakage phase, impacting stress leads to particle fragmentation below 45 µm. In the plateau phase, attrition results in ultrafine particles which eventually cause the formation of agglomerates. The computation of an average reference curve allowed the evaluation of single grinding trials for detection of possible deviations from the predicted course. This sensing technology is an important step towards higher reliability and reproducibility in sample preparation of powder material.

Key words

• **Sensory signal** • **Real time monitoring** • **Grinding** • **Grinding phases** • **Disc mill**

Introduction

Granular material is routinely pulverized in a disc mill before the chemical composition of the sample is analyzed by X-ray fluorescence (XRF) spectroscopy or other analytical methods. It is well known that the analytical precision and accuracy depends significantly on the correct performance of the grinding step in the disc mill. Minor variances in the particle size distribution after grinding may have a considerable impact on the XRF results leading to deviations of more than 30 % [1]. There are several factors potentially influencing the sample grain size in the course of the grinding process. These include grinding vessel overload, wear of the grinding set, blockage of the grinding set, inadequate efficiency of the grinding aid, significant divergence of sample properties like hardness, formation of agglomerates and others more. It is of prime importance to minimize the bias from these factors in order to reduce the total analytical error accumulating during sample preparation and analysis.

As we have shown previously the acceleration measurement of the grinding vessel enables the real-time assessment of the grinding process. The sensory signal does not only allow the graphical display of the grinding vessel movement (Figure 1) but also the evaluation of

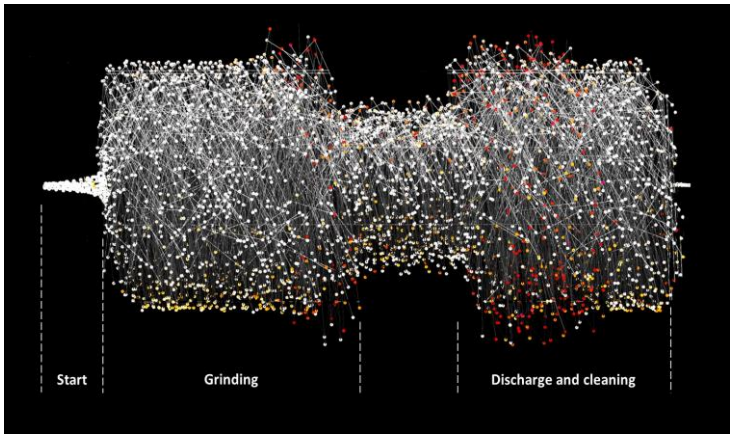

Figure 1: *Graphical display of acceleration values in x- and y- direction over time. In this example various stages of a typical grinding cycle are shown including start of the grinding process, the grinding itself as well as discharge of the material from the grinding vessel and cleaning of the grinding vessel. This application note focuses on the detailed assessment of the grinding phase.*

different key performance indicators relevant for the grinding process. Accordingly, we demonstrated that the approach is applicable for tool condition monitoring of the grinding set and swing aggregate [2, 3], predictive maintenance of bolt failure [4] and distinction between sufficient grinding and grinding failure [5].

In this study we will investigate whether the acceleration signal provides insights into the grinding processes themselves. More specifically, we will build a reference acceleration curve from single grinding trials which is characteristic for a specific sample material. Based on this acceleration curve we are aiming at identifying distinct grinding phases and their effect on the particle size distribution. Eventually, we will undertake initial tests to determine whether the reference acceleration curve of a specific material can be used to classify individual grinding trials and to determine whether they deviate from the predicted grinding process.

The relevant aspect of this study is that real-time monitoring of each single grinding trial would allow a seamless and more efficient control of the sample preparation process. This again would most likely have a beneficial influence on reliability and reproducibility of the analysis results.

Method

For this this study, we used the combined mill and press HP-MP (Herzog, Germany) equipped with a 100 ccm tungsten carbide vessel. Initially, we performed 3 trials without any sample material (empty grinding vessel) at rotation speed of 1400 rpm for 40 s.

Afterwards, we pulverized 30 g of clinker samples. We executed four different test protocols with 10 grinding trials each. The rotation speed (1400 rpm) and amount of grinding aid (cellulose and wax) were identical for all 40 grinding trials. According to the test protocol, the grinding time was either 30 s, 60 s, 90 s or 120 s. After completion of each grinding trial, the grain size distribution of the ground sample was determined using an air jet sieve with a mesh width of 45 µm.

In each trial we monitored the acceleration of the grinding vessel by a sensor mounted on the lower half of the swinging aggregate. The sensory signal was acquired by the PLC of the HP-MP and forwarded to the PrepMaster Analytics software for further data computation, graphical display and statistical analysis. Based on the acceleration values in x- and y- direction the root mean square (RMS) of acceleration was computed for each point of time resulting in an acceleration curve for each trial. Based on the 40 acceleration curves we calculated an average reference acceleration curve including the corresponding standard deviation. This mean average curve served as a reference curve for the subsequent single grinding trials.

Finally, we carried out four trials with 30 g clinker at a rotation speed of 1400 rpm for 120 s. The grain size distribution and the acceleration curve of each trial were compared to the reference curve built from the 40 previous trials.

Results

Acceleration curve of an empty grinding vessel

In a first step, we compared the RMS acceleration signal of an empty grinding vessel to the signal during grinding of clinker. The capture time for this test series was 40 s. The

acceleration curve of an empty grinding vessel showed a peak at 4 s with an RMS value of 61 m/s^2. Thereafter, the RMS decreased to a value of approx. 59 m/s^2 and remained constant afterwards (Figure 2, blue curve). In comparison, during grinding of clinker, the mean average acceleration curve showed clearly lower RMS values peaking around 56 m/s^2, transiently decreasing to 52- 53 m/s^2 and levelling off at 54-55 m/s^2 (Figure 2, black curve).

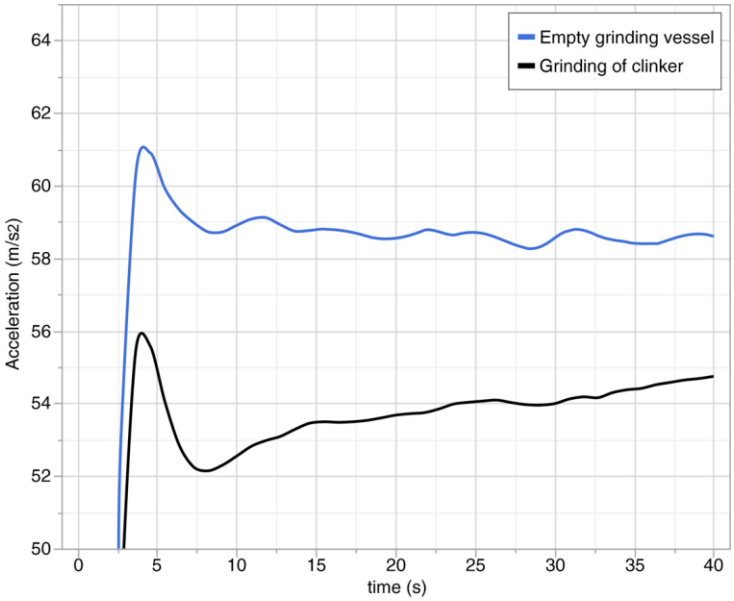

Figure 2: *Comparison of acceleration curve during motion of an empty grinding vessel (blue line) and during grinding of clinker (black line).*

Grain size distribution during grinding of clinker

The grinding process led to a significant reduction in grain size of the clinker sample. Before grinding, evaluation of the grain size distribution showed no particles below 45 µm (Figure 3, A). After 30 s of grinding, the portion of particle below 45 µm significantly increased to 87.0 ± 0.9 % (mean ± standard deviation). After 30 and 60 s of grinding, the sieve analysis showed relatively unchanged values with 89.2 ± 0.7 % and 88.1 ± 1.1 %, respectively. The microscopic inspection revealed a finely ground and homogeneous material (Figure 3, B). However, after 120 s of grinding, the grain size portion below 45 µm significantly decreased to 80.7 ± 1.2 %. This shift in the grain size distribution was due to the formation of agglomerates as illustrated by the microscopic image in Figure 3, C.

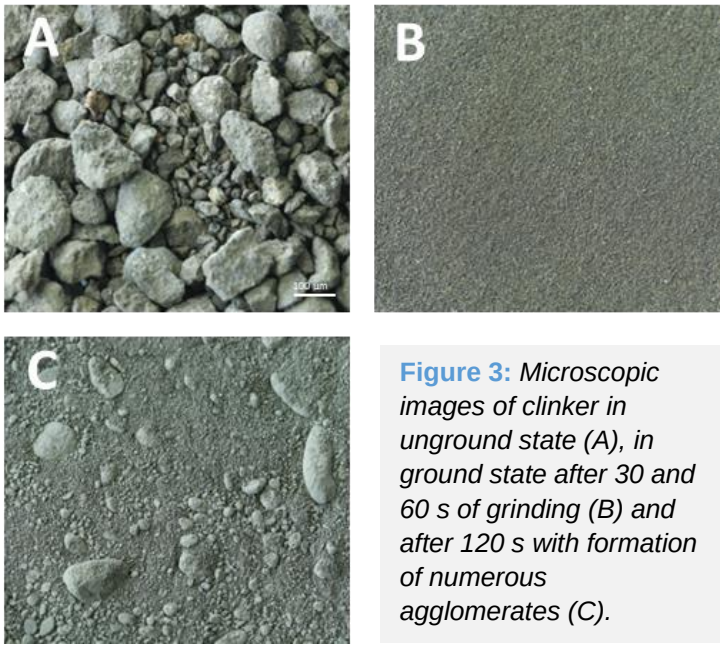

Figure 3: *Microscopic images of clinker in unground state (A), in ground state after 30 and 60 s of grinding (B) and after 120 s with formation of numerous agglomerates (C).*

Pattern of the grinding acceleration curve

The mean average acceleration curve computed from 40 grinding trials showed a specific pattern (Figure 4). In conjunction with the above mentioned grain size analysis, we identified three distinct phases in the course of clinker grinding. The first “breakage phase” lasted about 30 s and was characterized by a transient decrease of acceleration from approx. 54.5 m/s^2 to 53.0 m/s^2 and a subsequent increase to 54 m/s^2. At the end of the phase, the comminution of particles to sizes below 45 µm was almost completed as consecutive analyses did not yield significantly better results.

The second phase, the “plateau phase”, took about 60 s. Initially, the acceleration RMS value remained constant around 54.0 m/s^2 with only slight fluctuations. At the end of this phase, the curve showed a slightly sloping trend with a RMS reduction by approx. 0.3 m/s^2. The grain size analysis at 60 s and 90 s were not significantly different to the value at the end of the breakage phase.

The third phase, “agglomeration phase”, was characterized by a rapid and significant decrease of the acceleration by approx. 2.0 m/s^2. The drop in acceleration was accompanied by a decrease of the particles below 45 µm and an increase in agglomerates.

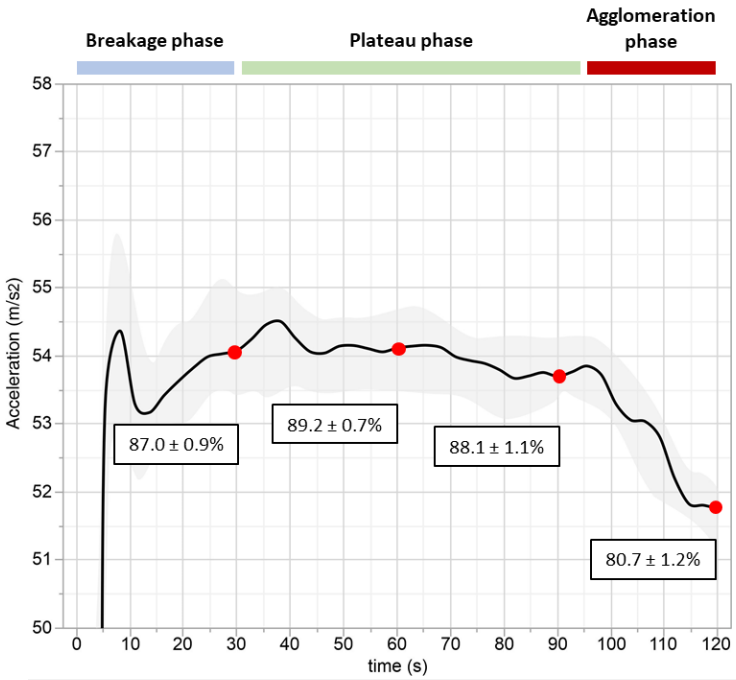

Figure 4: *Display of the average acceleration curve built from single trials during grinding of clinker. Within the boxes the % portion (± SD) of particles below 45 µm is indicated. The different phases are clearly distinguishable based on the acceleration curve.*

Comparison of single grinding trials with the mean average acceleration curve and grain size

The curve shape in each of the four individual grinding trials was similar to the average reference acceleration curve of the 40 previous grinding trials (Figure 5, A- D). Each individual curve was within the limit values of the reference curve formed by its standard deviation. Also, the grain size distribution values after 120 s of grinding were comparable to the mean average (79.5 %, 81.2 %, 81.4 %, 79.7 % vs. 80.7 ± 1.2 %).

Figure 5 (see below): *Projection of the acceleration curve of single grinding trials (red line) on the average reference curve (black line). The gray shaded area indicates the standard deviation of the reference curve. All acceleration curves of single grinding were within the borders of the reference curve. The grain size values (red boxes) were similar to the mean value of the reference curve (black box in A).*

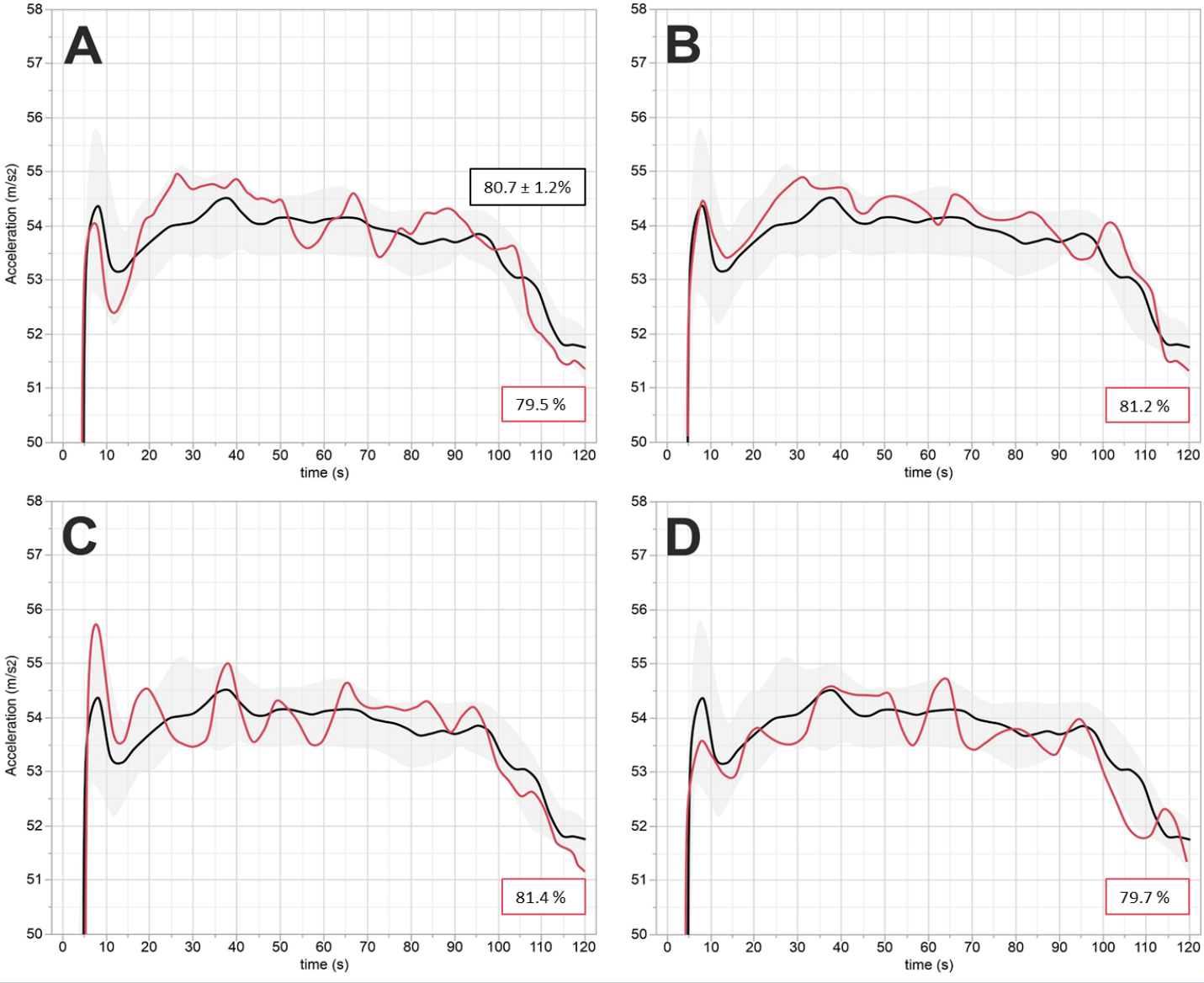

Discussion

There are three main conclusions that can be drawn from this study. First, the decrease of acceleration observed during grinding of clinker reflects the amount of energy necessary for comminution of sample particles. The decrease in acceleration corresponds to the conversion of the kinetic energy of the grinding vessel to the energy used for comminution of the sample particle. In contrast to this finding, we did not observe any larger decline of acceleration during motion of an empty grinding vessel. The most probable reason for this is that no kinetic energy was deducted for reduction of the sample grain size. The amount and course of the acceleration decline might be used for a quantitative assessment of the grinding process. Furthermore, the acceleration data might also reveal specific sample properties like, e.g., hardness, specific fracture energy etc. For a precise quantitative evaluation, other contributing factors will have to be considered like energy dissipation due to warm-up of the grinding vessel.

Second, the grinding process of clinker is characterized by three clearly distinguishable phases. The initial phase (breakage phase) causes majority of particles to be smaller than 45 µm. At this stage, the predominant mechanism of particle size reduction is impact breakage. Accordingly, the impacting stress energy is converted into elastic energy applied to lattice lacks within the particles. These lattice lacks may involve vacancies, dislocations, grain joints, etc. and give rise to cracking of particles [6]. At the end of the breakage phase, the fragmentation of particles is completed and the acceleration values rise again to reach a stable level.

In the second phase (plateau phase), particle size reduction still continues but is mainly based on attrition. While comminution due to breakage is characterized by formation of daughter fragments along preformed fracture lines of sample particles, attrition produces very fine particles directly without going through intermediate stages [7]. In this experimental setting we did not perform a grain size analysis by laser diffraction or image analysis to examine the grain size distribution below 45 µm. However, it is very likely that the plateau phase generates ultrafine particles in the range of 10 µm or less by scratching on the surface of the progenitor particles. The redistribution into the range of ultrafine particles leads to a continuous increase of the specific surface of the grinding product [8]. If the specific surface exceeds a critical value formation of agglomeration starts [9].

The beginning of the third phase (agglomeration phase) is clearly delimited from the previous plateau phase by a rapid drop in acceleration. The origin of the acceleration drop is yet unclear. The increase of the specific surface in the plateau phase most probably causes a significant enhancement of interparticle interaction attributed to Van der Waals forces, polar interactions and strong chemical forces [10]. The particle- particle forces initiate attractive interactions promoting the formation of aggregates and agglomerates. The drop in acceleration might be explained by a higher energy consumption triggered by the generation of large agglomerates out of smaller agglomerates. Alternatively, the acceleration loss might be caused by the energy necessary to destroy the agglomerates which are continuously built in the agglomeration phase. Further investigations are needed to clarify the exact underlying mechanism. In general, it remains to be noted that characteristic and duration of the three grinding phase may vary from material to material.

As a third conclusion from this study we found that the acceleration measurement allows the monitoring and verification of single grinding trials. The course of each acceleration curve can be compared to the expected acceleration course calculated from the mean average of previous trials. A significant discrepancy of a grinding trial can be automatically detected and raise a red flag in terms of reliability of subsequent analysis results of this sample. This would be an important step towards better

control and reproducibility of sample preparation resulting in a further reduction of the total analytical error.

In summary, the tool condition monitoring presented here has great potential to improve reliability and reproducibility of sample preparation of powder material. In forthcoming application notes we will demonstrate the possibilities that this smart industry solution offers for different applications.

References

[1] Mzyk Z., Baranowska I. and Mzyk J. (2002): Research on grain size effect in XRF analysis of pelletized samples, X-Ray Spectrom., 31: 39- 46

[2] HERZOG Application note 25/2020: Tool condition monitoring of disc mills- Monitoring of the proper swing aggregate function

[3] HERZOG Application note 26/2020: Tool condition monitoring of disc mills- Online monitoring of the wear of the grinding set

[4] HERZOG Application note 29/2020: Predicitive maintenance on disc mills using sensory signal monitoring

[5] HERZOG Application note 30/2020: Real-time monitoring of grinding efficiency in disc mills by acceleration monitoring

[6] Selim, KA and El-Rahiem FH (2014): On fragmentation and agglomeration phenomena in an ultrafine dry grinding process of the Egyptian calcium carbonate: the role of oleic acid addition, Journal of Mining World Express, 3:9-14

[7] Moothedath SK and Ahluwalia SC (1992): mechanism of grinding aids in comminution, Powder Technology, 71: 229- 237

[8] Guzzo, P., Tino A. and Santos J (2015): The onset of particle agglomeration during ultrafine grinding of limestone in a planetary ball mill, Powder Technology 284: 122- 129

[9] Prziwara P., Breitung- Faes S. and Kwade A. (2017): Impact of grinding aids on dry grinding performance, bulk properties and surface energy, Advanced Powder Technology, https://doi.org/10.1016/j.apt.2017.11.029

[10] Peukert W., Schwarzer HC, Stenger F. (2005): Control of aggregation in production and handling of nanoparticles, Chem. Eng. Process., 44: 245- 252

Germany

HERZOG Maschinenfabrik
GmbH & Co.KG
Auf dem Gehren 1
49086 Osnabrück
Germany
Phone +49 541 93320
info@herzog-maschinenfabrik.de
www.herzog-maschinenfabrik.de

USA

HERZOG Automation Corp.
16600 Sprague Road, Suite 400
Cleveland, Ohio 44130
USA
Phone +1 440 891 9777
info@herzogautomation.com
www.herzogautomation.com

Japan

HERZOG Japan Co., Ltd.
3-7, Komagome 2-chome
Toshima-ku
Tokio 170-0003
Japan
Phone +81 3 5907 1771
info@herzog.co.jp
www.herzog.co.jp

China

HERZOG (Shanghai) Automation Equipment Co., Ltd.
Section A2, 2/F, Building 6
No. 473, West Fute 1st Road,
Waigaoqiao F.T.Z., Shagnhai,
200131
P.R.China
Phone +86 21 50375915
info@herzog-automation.com.cn
www.herzog-automation.com.cn